

## Mo–V–Nb mixed oxides as catalysts in the selective oxidation of ethane

P. Botella<sup>a</sup>, J.M. López Nieto<sup>a,\*</sup>, A. Dejoz<sup>b</sup>, M.I. Vázquez<sup>b</sup>, A. Martínez-Arias<sup>c</sup>

<sup>a</sup> Instituto de Tecnología Química, UPV-CSIC, Avda. Los Naranjos s/n, 46022 Valencia, Spain

<sup>b</sup> Departamento de Ingeniería Química, Universidad de Valencia, Dr. Moliner 50, 46100 Burjassot, Spain

<sup>c</sup> Instituto de Catálisis y Petroleoquímica, CSIC, Campus Cantoblanco, 28049 Madrid, Spain

### Abstract

Mo–V–Nb–O mixed metal oxides, obtained by heat-treatment in N<sub>2</sub> at 425 °C, have been studied as catalysts in the oxidative dehydrogenation of ethane. They present higher catalytic activity, while maintaining the same selectivity to ethylene, than the corresponding metal oxides calcined under air. Both amorphous and crystalline phases are present on active and selective catalysts. The implications of the presence of these phases as well as their physicochemical characteristics on the nature of active and selective sites are discussed.

© 2002 Elsevier Science B.V. All rights reserved.

**Keywords:** Oxidation of ethane to ethylene; Oxydehydrogenation; Mo–V–Nb mixed oxides; Catalyst characterization (EPR, XRD, UV-Vis diffuse reflectance)

### 1. Introduction

High reaction temperature is generally used in the selective oxidation of short chain alkanes, especially ethane, as a consequence of their low reactivity [1–3]. For this reason, more active catalysts are required in order to decrease the reaction temperatures.

V-containing catalysts have been widely used in the oxidative dehydrogenation (ODH) of alkanes [1–3]. Mo–V–Nb mixed oxides have been proposed to be the most active and selective catalysts in the ODH of ethane at relatively low reaction temperatures (300–400 °C) [4–8]. However, the synthesis of acetic acid from ethane can also be favored by operating at low reaction temperature and/or with the incorporation of promoters [5,6,9].

The influence of both the preparation procedure and the composition of MoVNb catalysts on the ODH of ethane have been studied in the last years [4–8]. However, some discrepancies exist with respect to the nature of the crystalline phases in tested catalysts as well as on the active and selective sites for this reaction.

Mo<sup>5+</sup>–O and V<sup>4+</sup>–O are potentially the active sites in this reaction [4–9]. Thus, small amounts of acetaldehyde were only formed on Mo<sub>4</sub>O<sub>11</sub>–MoO<sub>3</sub>, whereas acetic acid was mainly observed on VO<sub>2</sub>. On the other hand, MoO<sub>2</sub> is itself very active but unselective for the formation of acetic acid. Thus, an improvement of the preparation of these catalysts would consist in avoiding the MoO<sub>2</sub>-like phases formation.

On the other hand, the amount of Mo<sup>5+</sup>–O and V<sup>4+</sup>–O species in the catalyst could be modified by applying changes in the catalyst composition and/or during the heat-treatment step. Accordingly to literature reports, the catalysts are generally prepared by evaporation of an aqueous solution and calcined in air

\* Corresponding author. Tel.: +34-96-38-77-808;

fax: +34-96-38-77-809.

E-mail address: jmlopez@itq.upv.es (J.M. López Nieto).

at 400 °C [1–8]. However, active and selective catalysts can also be achieved when the heat-treatment is carried out in an inert atmosphere [5,6].

In this paper we present, the influence of both the composition and the calcination conditions of Mo–V–Nb–O mixed oxides catalysts on their catalytic behavior in the ODH of ethane. We will show that the heat-treatment in N<sub>2</sub> can also be used for the preparation of active and selective catalysts.

## 2. Experimental

### 2.1. Catalyst preparation

The catalysts have been prepared from an aqueous solution of ammonium heptamolybdate, vanadyl sulfate and niobium oxalate. The aqueous solution was evaporated in rotavapor. The solids were dried at 100 °C overnight and, finally, heat-treated at 425 °C in N<sub>2</sub> during 4 h. Sample C was also heat-treated in N<sub>2</sub> at 600 °C for 2 h (sample C-6N) or calcined in air at 400 °C for 4 h (sample C-4A). Table 1 presents the composition of the catalysts.

### 2.2. Catalyst characterization

N<sub>2</sub> and Ar adsorption isotherms were obtained in an ASAP 2010 instrument at 77 and 87 K, respectively, after degassing the samples ( $1.33 \times 10^{-2}$  Pa) at 400 °C, overnight.

X-ray diffraction (XRD) patterns were collected using a Philips X'Pert diffractometer equipped with a graphite monochromator, operating at 40 kV and 45 mA and employing nickel-filtered Cu K $\alpha$  radiation ( $\lambda = 0.1542$  nm).

Diffuse reflectance UV-Vis spectra were collected on a Cary 5 equipped with a 'Praying Mantis' attachment from Harrick under ambient conditions.

Electron paramagnetic resonance (EPR) spectra were recorded at 77 K with a Bruker ER-200 spectrometer working at the X-band and calibrated with a DPPH standard ( $g = 2.0036$ ).

### 2.3. Catalytic tests

The catalytic experiments were carried out in a fixed bed quartz tubular reactor (i.d. 20 mm, length 400 mm), working at atmospheric pressure in the 340–400 °C temperature range [10]. Catalyst samples (0.3–0.5 mm particle size) were introduced in the reactor and diluted with 8 g of silicon carbide (0.5–0.75 mm particle size) in order to keep a constant volume in the catalyst bed. The flow rate and the amount of catalyst were varied in order to achieve different ethane conversion levels. The feed consisted of a mixture of ethane/oxygen/helium with a molar ratio of 30/10/60. Reactants and reaction products were analyzed by on-line gas chromatography [10]. A blank run showed that the homogeneous reaction could be neglected under our reaction conditions.

## 3. Results and discussion

### 3.1. Catalyst characterization

Small differences in the surface area were observed for samples heat-treated in N<sub>2</sub> (about 20–30 m<sup>2</sup> g<sup>−1</sup>). However, the sample calcined in air presented a surface area (14.3 m<sup>2</sup> g<sup>−1</sup>) lower than the corresponding

Table 1  
Characteristics and catalytic properties of MoVNb catalysts<sup>a</sup>

Catalyst	MoVNb atomic ratio	Conversion of ethane (%)	Yield of ethylene (%)	Selectivity (%)		
				C <sub>2</sub> H <sub>4</sub>	CO	CO <sub>2</sub>
A-4N	1–0.6–0	1.1	0.8	74.8	17.3	7.9
B-4N	1–0.3–0.12	11.4	7.3	64.0	27.1	8.9
C-4N	1–0.6–0.12	21.5	13.0	60.5	29.2	10.3
D-4N	1–0.9–0.12	15.7	7.2	45.9	41.2	12.9
E-4N	1–0.6–0.24	22.7	10.9	47.8	38.1	14.1
C-6N	1–0.6–0.12	5.8	3.4	58.0	27.2	14.8
C-4A	1–0.6–0.12	17.6	12.1	68.6	23.2	8.2

<sup>a</sup> Reaction conditions:  $W/F = 20.5$  g<sub>cat</sub> h mol<sup>−1</sup><sub>C<sub>2</sub></sub>;  $T = 400$  °C.

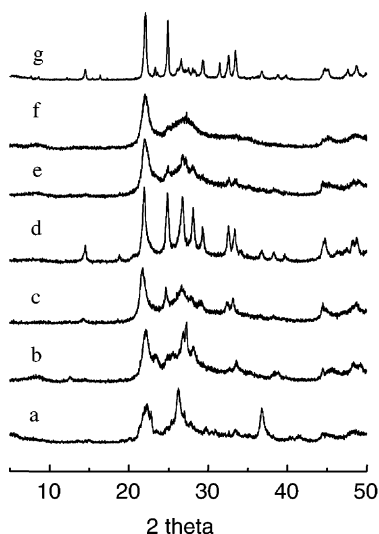


Fig. 1. XRD of MoVNb catalysts: (a) A-4N; (b) B-4N; (c) C-4N; (d) D-4N; (e) E-4N; (f) C-4A; (g) C-6N.

sample heat-treated in  $N_2$  ( $31.2 \text{ m}^2 \text{ g}^{-1}$ ). On the other hand, the sample heat-treated at  $600^\circ\text{C}$  presented a low surface area ( $<10 \text{ m}^2 \text{ g}^{-1}$ ).

Since small differences have been observed during oxidation–reduction cycles of MoVNb oxides [4–6], the characterization of catalysts was carried out after the catalytic tests.

The Nb-free sample shows the presence of  $\text{MoO}_2$  [JCPDS, 32-671] (reflections at  $2\theta = 26.3, 36.6$  and  $53.8$ ), in addition to a broad reflection at  $d = 4.0\text{--}3.9 \text{ \AA}$  ( $2\theta = 22\text{--}22.6^\circ$ ) (Fig. 1a). The broad peak can be related to the formation of a low crystalline Mo,V-containing phase and/or suboxides of  $\text{MoO}_3$  [4,5].

The incorporation of Nb increases the intensity of the reflection at  $4.0 \text{ \AA}$  (Fig. 1c). In addition, new reflections are observed at  $2\theta = 14.4, 24.7, 26.7$  (broad peak),  $28.15, 29.5, 32.65, 33.65, 44.7, 48.3$ , and  $48.8$  in sample C-4N (Fig. 1c). This could correspond to  $\text{Mo}_6\text{V}_9\text{O}_{40}$  [JCPDS, 34-0527] and  $\text{Mo}_4\text{V}_6\text{O}_{25}$  [JCPDS, 34-0530]. However, the intensities of these reflections decrease at higher Nb/Mo ratios (Fig. 1e). According to the literature [4–8], different V- and/or Nb-containing suboxides of  $\text{MoO}_3$  can be achieved. The fact that the intensities of the peaks observed in Fig. 1 (spectra c and e) change with the Nb/Mo ratio suggests that the amount of V or Nb incorporated in

the crystalline phase could be different for each catalyst. However, in many cases it is difficult to assign the nature of these crystalline phases since both V- and/or Nb-containing crystalline phases could give rise to very similar XRD patterns.

The XRD patterns of MoVNbO samples with different Mo/V atomic ratio are comparatively shown in Fig. 1 (spectra b–d). At low V/Mo ratio,  $\text{MoO}_3$  [JCPDS, 5-508] can be observed (Fig. 1b). In addition to this, both  $\text{Mo}_6\text{V}_9\text{O}_{40}$  and  $\text{Mo}_4\text{V}_6\text{O}_{25}$  are observed. The intensities of the corresponding peaks increase with the V/Mo ratio (Fig. 1d).

Fig. 1f shows the XRD pattern of sample C-4A (calcined at  $400^\circ\text{C}$  in air). This sample shows a XRD pattern similar to that observed in the corresponding sample heat-treated in  $N_2$  (Fig. 1c) although the intensities of the most important peaks were lower in the sample calcined in air.

Fig. 1g shows the XRD patterns of sample C-6N (heat-treated at  $600^\circ\text{C}$  for 2 h in  $N_2$ ). In addition to the reflections observed for the sample heat-treated at  $425^\circ\text{C}$  (see Fig. 1c) new reflections are observed at  $2\theta = 7.6, 8.6, 12.2, 13.8, 15.4, 16.4, 23.2, 23.5, 24.8, 27.4, 27.9, 28.2, 31.4$  and  $38.9$ , which corresponds to the formation of  $(\text{V}_{0.07}\text{Mo}_{0.93})_5\text{O}_{14}$  [JCPDS, 31-1437] and/or  $(\text{Nb}_{0.09}\text{Mo}_{0.91})\text{O}_{2.80}$  [JCPDS, 27-1310]. However, the formation of a  $\text{Mo}_{5-x}(\text{V/Nb})_x\text{O}_{14}$  crystalline phase cannot be completely ruled out [9]. So, the amorphous phase observed in samples heat-treated at  $425^\circ\text{C}$  could be the precursor of some of these crystalline phases.

Fig. 2 shows the diffuse reflectance UV-Vis spectra of samples after the catalytic tests. Important differences can be observed depending on the composition and/or the heat-treatment conditions. All samples present two broad bands. The first band, in the  $200\text{--}450 \text{ nm}$  region, can be related to the presence of  $\text{Mo}^{6+}$ ,  $\text{V}^{5+}$  and  $\text{Nb}^{5+}$  species with different environment [11,12]. The second band, in the  $500\text{--}700 \text{ nm}$  region, is related to the presence of  $\text{Mo}^{5+}$  ( $550\text{--}590 \text{ nm}$ ) and  $\text{V}^{4+}$  ( $600\text{--}650 \text{ nm}$ ) [11]. In addition, a band at  $400 \text{ nm}$  increases with the v/Mo ratio. This can be ascribed to  $\text{V}^{5+}$  species in an octahedral coordination [13].

Moreover, the intensity of the band at  $650 \text{ nm}$  increases with the Nb/Mo ratio (Fig. 2d). This could correspond to the reduction of  $\text{V}^{5+}$  species with oxalate anions during the catalyst preparation. Accord-

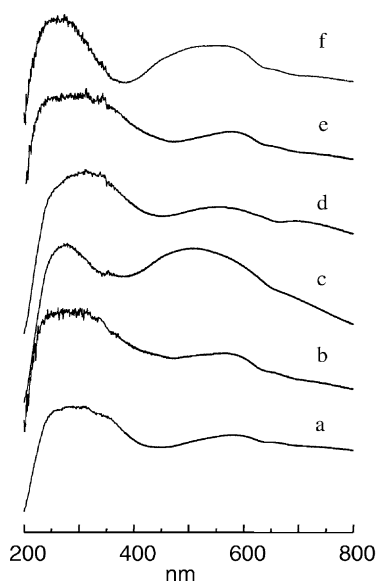


Fig. 2. Diffuse reflectance (UV-Vis) spectra of MoVNb catalysts: (a) B-4N; (b) C-4N; (c) D-4N; (d) E-4N; (e) C-4A; (f) C-6N.

ingly, the amount of reduced species is low when the amount of oxalate anions employed during the sample synthesis is low.

Fig. 3 shows the EPR spectra of the samples A-4N (Fig. 3a) and C-4N (Fig. 3b). The spectra are mainly constituted by axial signals with  $g_{\perp} = 1.979$ – $1.962$  and  $g_{\parallel} = 1.895$ – $1.890$  with varying average line widths. The EPR parameters and spectral shapes observed are consistent with attribution of these signals to  $\text{Mo}^{5+}$  (in the oxomolybdenum form) species

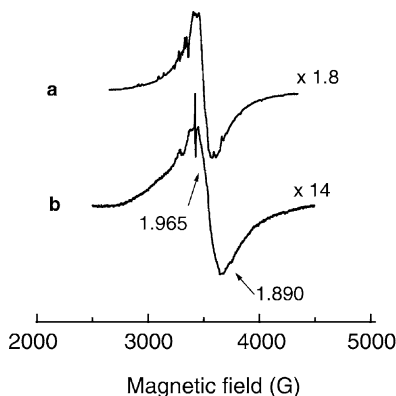


Fig. 3. EPR spectra of A-4N (a) and C-4N (b) samples.

in distorted octahedral environments [14]. Superimposed on that signal, it can be observed the presence of sharp features, most likely arising from the hyperfine structure of minor isolated  $\text{V}^{4+}$  species present in that sample. The relatively large widths of the signals and the absence of a clear resolution of hyperfine features in them indicates that the paramagnetic centers are immersed into magnetically active environments where they are subjected to relatively strong spin–spin interactions. Quantitative determination of the amount of paramagnetic species in these spectra yields values of 181.5 and  $30.1 \mu\text{mol g}^{-1}$  for samples A-4N and C-4N, respectively.

### 3.2. Ethane oxidation

Table 1 shows the catalytic results obtained during the oxidation of ethane at  $400^{\circ}\text{C}$ . Ethylene, CO and  $\text{CO}_2$  were the main reaction products. Acetic acid was also observed, as traces, at high conversion levels. These results suggest that the conversion of ethane increases initially with the V-content, presenting a maximum for sample C-4N ( $\text{Mo}_1\text{V}_{0.6}\text{Nb}_{0.12}$ ). On the other hand, the Nb-containing samples showed higher catalytic activity than the Nb-free sample. Thus, it appears that the catalytic activity is related to the presence of V-atoms, although the incorporation of Nb presents a positive effect on the catalytic activity.

Fig. 4 shows the variation of the selectivity to ethylene with the ethane conversion obtained during the oxidation of ethane at  $340$ – $400^{\circ}\text{C}$  on samples with different V- (Fig. 4a) or Nb-contents (Fig. 4b). In all cases, the selectivity to ethylene decreases with the ethane conversion, although sample C-4N presents both the highest initial selectivity to ethylene (at low ethane conversions) and the lowest ethylene decomposition (at high ethane conversions).

Fig. 5 shows the variation of the selectivities to the main reaction products achieved on samples C-4N and C-4A. It can be seen that both samples present similar selectivities to ethylene. However, as it can be observed in Fig. 6, the sample heat-treated in  $\text{N}_2$  (C-4N) presented a relatively higher yield of ethylene than the corresponding sample calcined in air (C-4A), at the same reaction conditions.

It appears that the atmosphere used during the heat-treatment step can slightly modify the catalytic activity of these catalysts. Although both catalysts

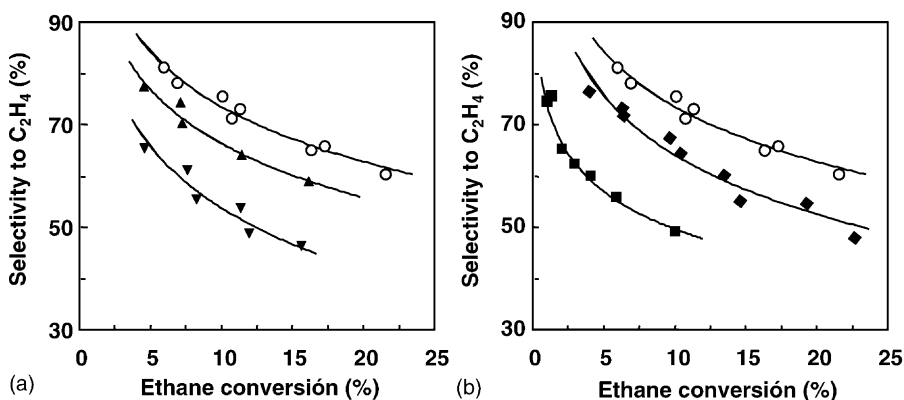


Fig. 4. Variation of the selectivity to ethylene with the ethene conversion during the oxidation of ethane on Mo-V-Nb catalysts with different V- (a) or Nb-contents (b). Symbols: A-4N (■); B-4N (▲); C-4N (○); D-4N (▼); E-4N (◆).

present similar XRD after the catalytic tests (Fig. 1), it should be indicated that MoO<sub>3</sub> was scarcely observed after the calcination in air while it was not observed during the heat-treatment in N<sub>2</sub>. So, the calcination in air could favor the achievement of undoped Mo-oxides with higher crystallinities, which could lead to a lower catalytic activity. These results are apparently in trouble with those previously reported [4,5], who appointed that the materials heat-treated in N<sub>2</sub> presented lower catalytic performance than those calcined in air. At this point, one should consider that differences in the catalyst preparation and elemental composition (especially V-content) can also influence the formation of Mo-V-Nb-containing phases during the heat-treatment step.

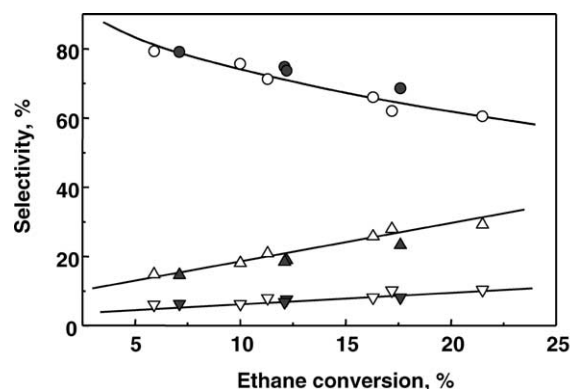


Fig. 5. Variation of the selectivity to the main reaction products, i.e. ethylene (○, ●), CO (△, ▲) and CO<sub>2</sub> (▽, ▼) with the ethane conversion obtained during the ODH of ethane on C-4N (○, △, ▽) and C-4A (●, ▲, ▼) catalysts.

On the other hand, the results presented in Figs. 4 and 5 suggest that the effects of catalyst composition on catalyst activity and selectivity could be explained in terms of Scheme 1, in agreement to previous papers [1–3,15]. Ethane can be transformed either through

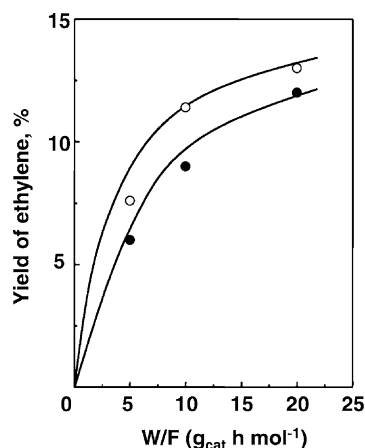
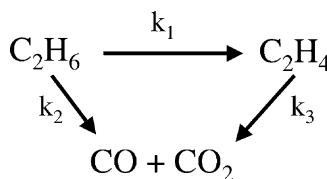


Fig. 6. Variation of the yield of ethylene with the contact time,  $W/F$  (in  $\text{g}_{\text{cat}} \text{h mol}_{\text{C}_2\text{H}_6}^{-1}$ ), obtained during the ODH of ethane at 400 °C on C-4N (○) and C-4A (●) catalysts.



Scheme 1. Reaction network in ODH of ethane.

ODH to form ethylene or by combustion to form CO and CO<sub>2</sub>, whereas ethylene can be transformed to CO<sub>x</sub> (especially CO). Although all the catalysts presented high initial selectivities to ethylene (at zero ethane conversion), the selectivities to ethylene and the extension of the deep oxidation of ethylene strongly depend on the catalyst composition.

According to these results, V<sup>5+</sup> species seem to be the active sites in ethane activation in both Nb-free and Nb-containing catalysts. The incorporation of Nb favors both higher catalytic activities and higher selectivities to ethylene. In this way, higher surface areas were achieved in Nb-containing samples. In addition, the incorporation of Nb leads to the elimination of MoO<sub>2</sub> favoring higher selectivities to ethylene.

On the other hand, the role of Mo<sup>5+</sup>/Mo<sup>6+</sup> species is still unclear. However, they are involved in the formation of V- and Nb-containing crystalline phases that facilitate the presence of isolated sites [16].

In conclusion, active and selective MoVNbO catalysts can be achieved by calcination at about 400 °C of the corresponding mixed metal oxides. N<sub>2</sub> or air can be used during the heat-treatment step although in the first case a higher yield of ethylene per gram of catalyst can be achieved. This is probably a consequence of the higher amount of Mo<sup>5+</sup> species and the higher interaction of molybdenum oxides with V and Nb ions which seem to be favored when the heat-treatment is carried out in N<sub>2</sub> at relatively low temperature (425 °C). However, low active catalysts have been achieved at high heat-treatment temperatures, in which new crystalline phases have been found.

## Acknowledgements

Financial support by the Spanish DGICYT (PPQ-2000-1396) is gratefully acknowledged. Thanks are due to Prof. J. Soria for the use of the EPR spectrometer.

## References

- [1] T. Blasco, J.M. López Nieto, *Appl. Catal. A* 157 (1997) 117.
- [2] F. Cavani, F. Trifiró, *Catal. Today* 24 (1995) 307.
- [3] M. Bañares, *Catal. Today* 51 (1999) 319.
- [4] E.M. Thorsteinson, T.P. Wilson, F.G. Young, P.H. Kasai, *J. Catal.* 52 (1978) 116.
- [5] M. Mezourki, B. Taouk, L. Monceaux, E. Bordes, P. Courtine, *Stud. Surf. Sci. Catal.* 72 (1992) 165.
- [6] M. Mezourki, B. Taouk, L. Tessier, E. Bordes, P. Courtine, *Stud. Surf. Sci. Catal.* 75 (1993) 753.
- [7] O. Desponds, R.L. Keiski, G.A. Somorjai, *Catal. Lett.* 19 (1993) 17.
- [8] K. Ruth, R. Kieffer, R. Burch, *J. Catal.* 175 (1998) 16; K. Ruth, R. Kieffer, R. Burch, *J. Catal.* 175 (1998) 27.
- [9] D. Linke, D. Wolf, M. Baerns, O. Timpe, R. Schölgl, S. Zeyß, U. Dingerdissen, *J. Catal.* 205 (2002) 16.
- [10] B. Solsona, T. Blasco, J.M. López Nieto, M.L. Peña, F. Rey, A. Vidal-Moya, *J. Catal.* 203 (2001) 443.
- [11] V.R. Porter, W.B. White, R. Roy, *J. Solid State Chem.* 4 (1972) 250.
- [12] X. Gao, I.E. Wachs, M.S. Wong, J.Y. Ying, *J. Catal.* 203 (2001) 18.
- [13] T. Blasco, P. Concepción, J.M. López Nieto, J. Pérez-Pariente, *J. Catal.* 152 (1995) 1.
- [14] K. Dyrek, M. Che, *Chem. Rev.* 97 (1997) 305.
- [15] M.D. Argyle, K. Chen, A.T. Bell, E. Iglesia, *J. Phys. Chem. B* 106 (2002) 5421.
- [16] J.C. Volta, *Top. Catal.* 15 (2001) 121.